ATLANTIS PRESS
Advances in Engineering Research, volume 202
Proceedings of the International Conference on Sustainable Biomass (ICSB 2019)

The Technical Concept of Differential Optical Absorption Spectroscopy for SO_2 Gas Spectrum Monitoring on Volcanic Ash of Gunung Anak Krakatau volcano

Ardian Ulvan[1] Muhamad Rifky Maulana[1] Mona Arif Muda Batubara[1]

Nora Aditiyan[1] Melvi [1,*]

[1] *Department of Electrical Engineering, Universitas Lampung*
[*] *Corresponding author. Email: melvi@eng.unila.ac.id*

ABSTRACT
Gunung Anak Krakatau is one of the active volcanoes in Indonesia. In October – December 2018, it erupted 156 times by releasing incandescent materials and toxic gases in the form of sulphur dioxide (SO_2), carbon dioxide (CO_2), and hydrogen sulphide (H_2S) at 2 km radius. The release of SO_2 gas indicates that magma is approaching the surface and puts the volcano on alert status. Finally on 22 December 2018 the continued eruption caused the flank collapse on some part of the volcano, triggered a tsunami that stroke the coastal of Lampung and Banten. This work investigated the SO_2 gas monitoring technology using Differential Optical Absorption Spectroscopy (DOAS). The study specifically concerns on the working principles of DOAS, optimization of DOAS with optical bandpass filters and amplifiers, as well as the implementation architecture design of DOAS from Gunung Anak Krakatau Volcano to Hargo Pancuran Monitoring Station. Based on this study, the DOAS can be used to monitor SO_2 gas by using a catadioptric telescope and the optimization works for UG11 as an optical bandpass filter and Raman Amplifier as the amplifier.

Keywords: *Krakatau, Krakatoa, DOAS, volcanic ash, SO_2, early warning system*

1. INTRODUCTION

When an active volcano erupts, it spews ashes, rocks, and flows lava and landslides on the side of the volcano. Among the volcanic processes which are important are continuous gas emissions. In general, active volcanoes around the world continuously emit water vapor (H_2O) which is consolidated with heavy metals, carbon dioxide (CO_2), and sulphur dioxide (SO_2). In smaller amounts, the type of gas produced contains carbon monoxide (CO), hydrogen sulphide (H_2S), carbonyl sulphide (COS), carbon disulphide (CS_2), hydrogen chloride (HCl), hydrogen (H_2), methane (CH_4), hydrogen fluoride (HF), boron hydrogen bromine (HBr), and mercury (Hg) [1].

The indicators of an eruption are generally divided into 4 levels, namely the normal, alert, standby, and beware levels. Alert status signifies increased volcano activity. Standby status indicates increased volcano activity beyond the alert level, can be seen firsthand, and potentially an eruption. Beware status indicates the volcano will soon erupt. The release of SO_2 gas is considered an increase in volcano activity and indicates that magma is rising, making the volcano in a state of alert.

Gunung Anak Krakatau (GAK) is one of the active volcanoes in Indonesia, which is the volcanic remnant of Krakatau volcano. Since the eruptions that caused the flank collapse of the western side of the GAK that triggered the tsunami on 22 December 2018, the activity status of the volcano is at Level II (alert). Before the flank collapse the number of eruptions have reached 156 times on Wednesday, October 3 2018. According to the Central of Volcanology and Disaster Mitigation (*Pusat Vulkanologi dan Mitigasi Bencana Geologi* - PVMBG) of the Geological Agency, the GAK eruption burst the incandescent material within the radius of 2 kilometers. PVMBG also appealed to the people of Banten and Lampung Provinces and tourists to remain calm and not enter the exposed areas within a 2 kilometres radius [2]. As the effect of the eruption, the volcano emitted poisonous gases in the form of sulphur dioxide (SO_2), carbon dioxide (CO_2), and hydrogen sulphide (H_2S). On December 28, 2018, Gunung Anak Krakatau Volcano was on Standby level because it released the gas within a radius of 1 to 5 km. This condition should be responded by the stakeholders to provide technology that can monitor volcano activities with a safe, flexible distance, and implementing an early warning system in order to mitigate the incoming disaster.

The technology for monitoring volcano activity that has been implemented includes 6 sensors around Anak Krakatau Volcano (3 in Sumatra and 3 in Java) to anticipate the possible volcanic eruptions [3]. Another technology applied is the water level sensor installed on Sebesi Island for the water level as well as data to determine early warnings when a tsunami occurs in the Sunda Strait due to a tectonic or volcanic earthquake [4].

This work studied a SO_2 gas monitoring system and provide an architectural design of the monitoring system from GAK to the volcano monitoring station at Hargo Pancuran village, using Differential Optical Absorption Spectroscopy (DOAS). This technology is based on spectroscopy which uses ultraviolet (UV) light media to calculate the quantity of SO_2 gas in the atmosphere with a distance about 42 km (as seen in Figure 1), using an optical telescope, then sends the light through an optical fiber to a USB spectrometer to be processed and measured.

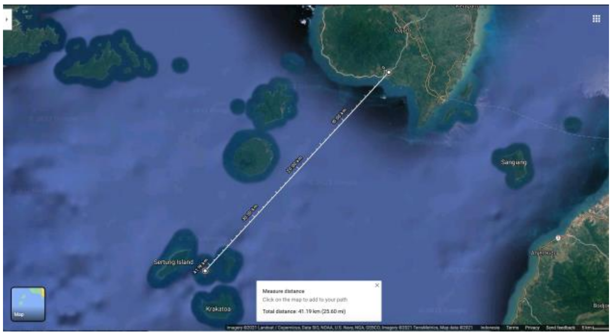

Figure 1 Line of sight distance between GAK and vulcano monitoring station at Hargo Pancuran.

2. RELATED WORKS

Differential Optical Absorption Spectroscopy, or DOAS, is a technology used to determine concentrations and analyze the spectrum of atmospheric species. The main approach of DOAS is to eliminate fluctuations in the recorded spectrum resulting from the scattering of molecules and aerosols in the atmosphere. The technique used in DOAS is to obtain a spectrum of the atmosphere with and without emissions. In terms of volcanic ash emissions, this can be achieved by collecting "lowland" or "clear sky" spectra from both sides of the volcanic ash [6]. Bo Galle and Manne Kihlman from Chalmers University have designed and developed the DOAS system [7]. Platt and Stutz conducted a spectrum analysis and determined the abundance of trace gases using the DOAS methodology [8]. Yan Zhang, in his thesis, applied the DOAS system to monitor the SO2 gas content in the volcanic ash of Mount Etna, Italy [9].

3. METHOD

3.1. The Functionality of DOAS

SO_2 gas is a poisonous gas that has a bad impact on humans, including irritation to the skin, eyes and respiratory system. This irritation can occur with SO_2 levels of 1 to 5 parts per million (ppm). This gas also has a spectrum wavelength in the range 270-317 nm. The wavelength region is in the UV category. This wavelength range makes SO_2 gas easy to monitor with DOAS technology as an object for which its concentration and intensity are calculated [5]. Based on the spectrum, DOAS technology cannot monitor CO_2 and H_2O gases because both has a wavelength range in millimetre to micrometre, while DOAS detection capabilities are in the nano meter range.

The basic equation for spectroscopic absorption is the Beer-Lambert Law. This law states, when a light beam passes through the homogeneous medium, then the light beam (I_0) will be absorbed (I_A) reflected (I_R), and transmitted (I_T). So that $I_0 = I_A + I_R + I_T$. In actual calculations, the I_R value is very small and is considered non-existent, so that $I_0 = I_A + I_T$.

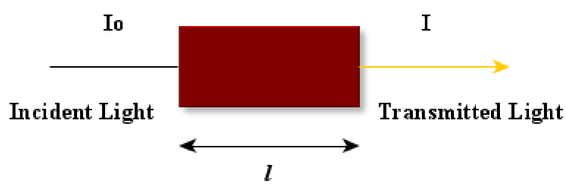

Figure 2 Basic scheme of absorption spectroscopy

Figure 2 is a simple example of Beer Lambert's Law. If the intensity of light transmitted is influenced by the molecular density of a species, the derivative of the formulas is as follow:

$$I(\lambda) = Io(\lambda)e^{-l\sigma(\lambda)n} \quad (1)$$

$$\tau(\lambda) = ln\frac{Io(\lambda)}{I(\lambda)} = L \sum_i \sigma i'(\lambda)ni \quad (2)$$

DOAS can be used with two techniques, namely active and passive technology. Active DOAS uses artificial light such as a thermal or laser light source on the DOAS transmitter device and shoots the light at the DOAS receiver through the gas you want to monitor, and the concentration is calculated. Meanwhile, passive DOAS utilizes wavelengths of sunlight or the moon, with a range of 100 nm to 1 mm so that it contains UV (100-400 nm), visible (400-770 nm), and infrared (770 nm - 1 mm) lights [10]. Figure 2 shows the active and passive DOAS techniques.

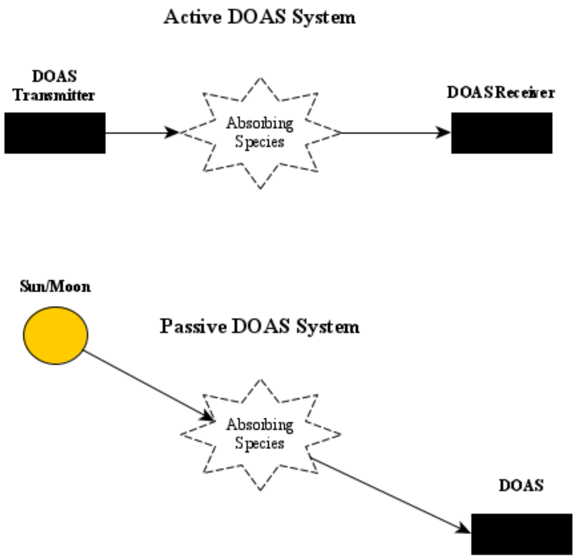

Figure 3. Active and passive DOAS techniques

The gas to be monitored, detected, or quantified by DOAS must be in the UV to visible wavelength range (200-770 nm). With the wavelength of SO_2 gas and the only gas in volcanic ash that is in the 200-770 nm range, makes SO_2 gas is able to be monitored by DOAS.

The components of the DOAS consist of an optical telescope, optical fiber and optical spectrometer. Optical telescopes are used to collect and focus light, including the electromagnetic spectrum to create clear images, live views, and collect sensor data. DOAS optical fiber guides the light waves from the telescope to the spectrometer. The optical spectrometer is used to separate and measure the light intensity or wavelength of the sun which is absorbed, passed, and ignored by the volcanic ash of the GAK, in this case is SO_2 gas. The detailed drawings and workings of the DOAS components are presented in the results and discussion section.

3.2. Proposed Implementation Architecture

Originally, the existing DOAS described in [6-9] is available without any treatment on light processing such as optical bandpass filters and optical amplifiers on the optical fiber. In this work, we introduce the deployment of bandpass filter and optical amplifier to improve the accuracy of the detector reading on the spectrometer. The implementation architecture is proposed as depicted in Figure 4.

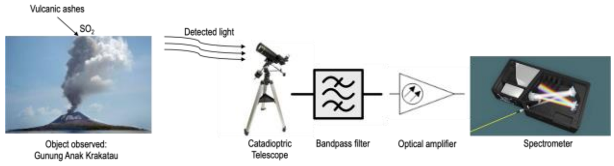

Figure 4. The implementation of DOAS to monitoring the volcanic activity of Gunung Anak Krakatau.

3.3. Deployment of Bandpass Filter

The proposed optical bandpass filter should has an upper and lower limit in accordance with the SO_2 gas spectrum, namely 270-317 nm. UG11 filter is the most suitable optical bandpass filter for this specification. Furthermore, several parameters related to the deployment of bandpass pass filter i.e., central wavelength (CWL), the full width at half maximum light transmission (FWHM), the absorbance/optical density (OD), and the maximum transmission of light (T) can be examined by equation 3:

$$CWL = \frac{\lambda 2 + \lambda 1}{2} \qquad T = 10^{-OD} \times 100$$

$$FWHM = \lambda_2 - \lambda_1 \qquad OD = -\log\left(\frac{T}{100}\right) \tag{3}$$

3.4 Deployment of Optical Amplifier

The optical amplifier is used to strengthen the wavelength of SO_2 detected by the telescope before being processed by the spectrometer. To improve the accuracy of the detector reading on the spectrometer, we introduce the use of dedicated optical amplifier. In this work, we determined intensely three types of optical amplifier, i.e., Semiconductor Optical Amplifier (SOA), Doper Fiber Amplifier (DFA), and Raman Amplifier, to attain the most suitable and comply with the purpose.

The SOA uses semiconductors to provide a reinforcing medium. This amplifier has a structure similar to the Fabry-Perot laser diode with the addition of an anti-reflection design element on the surface. The SOA scheme can be seen in Figure 5.

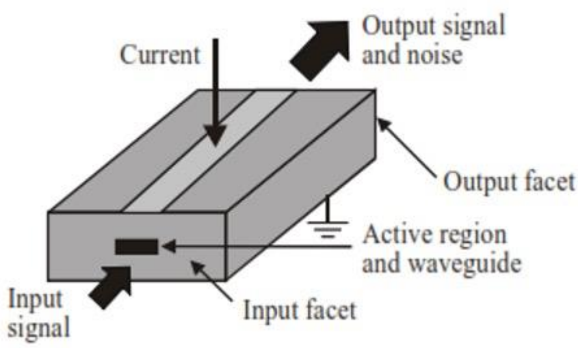

Figure 5. Optical signal amplification with SOA [11]

In the meantime, the DFA uses the in operation optical fibers as the amplification medium to amplify optical signals by pumping the particular photons as the dope (e.g., Erbium photons). The signal to be amplified and pumped photons are multiplied into the treated fiber, thus the signal is amplified through interaction with doping. The amplification of the signal on the DFA can be seen in the Figure 6.

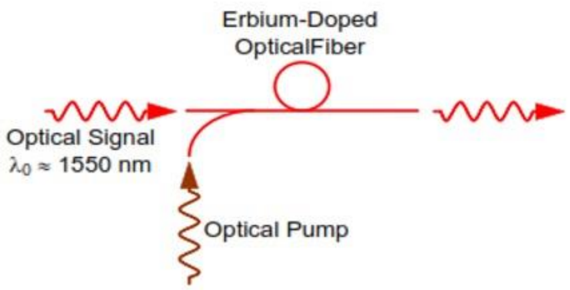

Figure 6. Optical signal amplification with DFA [11]

The last optical amplifier that has been examined for this project is the Raman amplifier. Raman Amplifier amplifies the signal by sending power from an external optical pump to the optical signal through a nonlinear optical process, as shown in Figure 7.

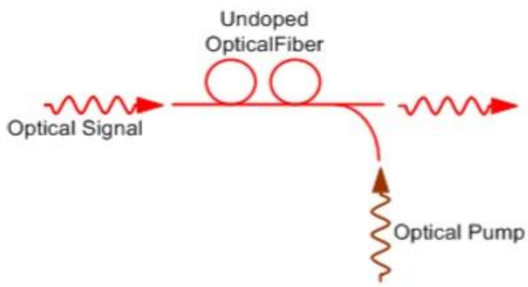

Figure 7. Signal amplification with Raman Amplifier [11]

Based on our study, we found that DFA and SOA have better amplification capabilities than Raman Amplifier. However, DFA can only amplify the wavelength in a certain range (1528-1605 nm). Meanwhile, SOA has a quite complicated way of working due to its nature to proceed the amplification in electrical domain that required for converting the optical signals into electric signals before the amplification process. In addition, SOA also amplifies the wavelength in the 1.3 - 1.5 μm range, not in the light waves (nm) range, especially the UV range. For that reason, then Raman Amplifier is preferred to be deployed due to its advantages that can amplify the spectrum over any range of the light wave.

4. RESULT AND DISCUSSION

4.1. The Absorption Phase of the Sun's Light Wavelength by Volcanic Gases

In this phase, the spectrum of sunlight in the range 100 nm - 1 mm, as I_0 (λ), passes through several volcanic gases of the GAK (σ), with a certain density (n), at a certain gas coverage length (l), so that it occurs. the absorbance or transmittance process (τ). The process in this phase is related to the equations 1 and 2 at the Section 2, with the following details.

The average solar radiation intensity of I_0 (λ) in Hargo Pancoran can be estimated by the intensity of solar radiation on the location of South Lampung, namely 5,234 W/m^2 [12]. The length of the SO_2 gas path from the GAK (l) is assumed to be 400 m based on the current volcano crater width. The value of σ (270-317 nm) is assumed to be 0.5 x 10^{-18} to 1.5 x 10^{-18} cm^2/molecule, as the mean value of the cross section of SO_2 gas absorption at room temperature of 295° K [13]. The total gas density of SO_2 (n) is 41.03 x 10^{-6} molecules/cm^3 as a general rule. With these assumed values, equation 1 which is used to determine the intensity that comes out of SO_2 gas becomes:

$$I(\lambda) = Io(\lambda)e^{-l\sigma(\lambda)n}$$

$$I\,(270) = 5.234\; e^{-40000\,x\,o{,}5\,x\,10^{-18}\,x\,41{,}03\,x\,10^{-6}}$$
$$I\,(270) = 5.234 \text{ W/m}^2$$

$$I\,(317) = 5.234\; e^{-40000\,x\,1{,}5\,x\,10^{-18}\,x\,41{,}03\,x\,10^{-6}}$$
$$I\,(317) = 5.234 \text{ W/m}^2$$

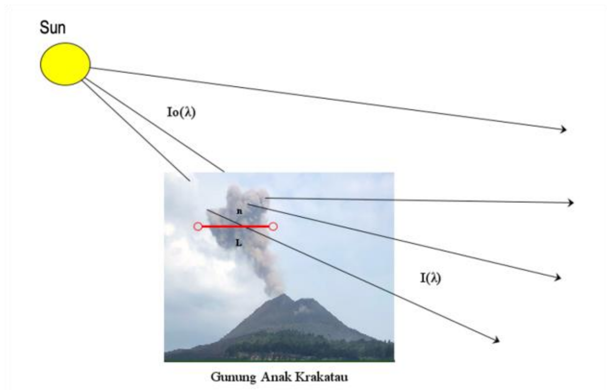

Figure 8. Phase 1, absorption of the sun's light spectrum by volcanic gases

The value above shows that the value of I (λ) is equal to I_0 (λ) when using the mean value of the cross section of SO_2 gas absorption (λ_1 = 270 nm, σ_1 = 0.5 x 10^{-18} cm^2/molecule and λ_2 = 317 nm, σ_2 = 1.5 x 10^{-18} cm^2/molecule) at room temperature 295° K and the gas path length as the assumed value. Based on the results of the equation also, it can be concluded that the smaller the value of the gas path length and the absorption cross section value until it approaches zero (smaller or equal to 10^{-10}), the value of I (λ) will increasingly equal I_0 (λ). As for equation 2 to determine the absorbance or transmittance with the same assumed value for the length of the gas path and the value of the cross section of gas absorption, then:

$$\tau(\lambda) = ln\frac{Io(\lambda)}{I(\lambda)}$$

$$\tau(270) = \tau(317) = ln\frac{5.234}{5.234} = 0$$

The entire phase 1 process is depicted in Figure 8.

4.2. Volcanic Gas Spectrum Collection Phase by Optical Telescope

In the second phase, various variations of volcanic gas wavelengths of GAK that have passed through the sun's light are captured by the telescopes. The ideal type of optical telescope needed to collect the wavelengths is chosen by considering the following aspects:

a. *Chromatic aberration*. This aberration occurs due to differences in the focus and refractive index of the lens when capturing many colours, resulting in the appearance of shadows with different distances. Refractor telescopes generally have this disadvantage but can be overcome by adding a correcting lens behind the objective lens.

b. *Spherical aberration*. This aberration occurs due to the curvature of the lens or mirror, resulting in the formation of an image that is not in accordance with the theory of reflection or refraction. Spherical aberration is a common drawback of many optical telescopes. As for the type of catadioptric telescope, it has a fairly good level of corrector in overcoming these shortcomings.

c. *Cost*. The catadioptric telescope is the most expensive type of telescope compared to the reflector and refractor telescopes, with the same specifications, especially on the aperture size.

d. *Design*. The telescope's design for capturing UV light is based on some previous research. Generally, optical telescopes are not made to capture UV light, because the earth's atmosphere can absorb the UV spectrum rapidly. As for some studies that require UV optical telescopes, they need them for monitoring at a relatively close distance, such as previous DOAS studies. The type of optical telescope used in this study is a catadioptric, because this type has the best correcting lens for researchers to overcome aberrations in processing UV light [14].

Based on the four points above, catadioptric telescopes have the best ability to process light, and have been used quite widely in several studies, although they are relatively expensive. Therefore, we propose the use of a catadioptric telescope for monitoring the SO_2 gas of the GAK. The entire phase 2 process is depicted in Figure 9.

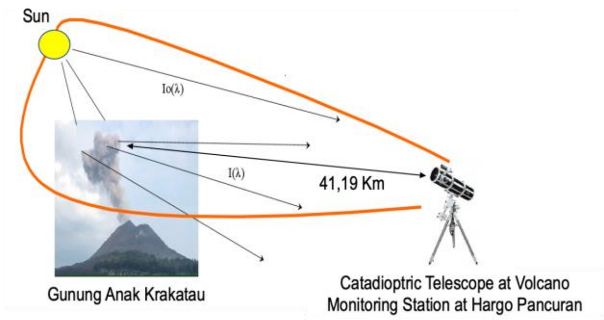

Figure 9. Phase 2, collecting the wavelengths of volcanic gas by an optical telescope

4.3. Transmission Phase of the Spectrum from the Optical Telescope to the Spectrometer

In the third phase, the wavelengths of GAK volcanic gas which is collected by the telescope, are sent to the spectrometer using the optical fiber cable. In this phase, we optimised the system by introducing an optical bandpass filter and an optical amplifier to improve the quality of the SO_2 wavelength, so that it is easier to be detected by the detector on the spectrometer. The proposed optical bandpass filter is the UG11 optical glass filter with the operational range of 254 - 365 nm, by which the range includes SO_2 gas wavelengths [15]. With a cut-on value of λ_1 = 254 nm and a cut-off value of λ_2 = 365 nm, as well as the OD or τ value obtained from the previous calculation of equations (1) and (2) = 0, then the equation (3) is used to find out the CWL, FWHM, and T as follow:

$$CWL = \frac{\lambda 2 + \lambda 1}{2} = \frac{365 + 254}{2} = 309{,}5 \text{ nm}$$

$$FWHM = \lambda_2 - \lambda_1 = 365 - 254 = 111 \text{ nm}$$

$$T = 10^{-OD} \times 100 = 10^0 \times 100 = 100\%$$

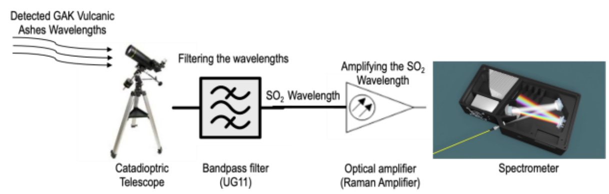

Figure 10. Phase 3, sending the spectrum from the telescope to the spectrometer.

After being filtered by the optical band pass filter, the wavelength is amplified by the Raman Amplifier. The special type of the proposed Raman Amplifier is a fused silica and nanosecond-laser-pump. This type can amplify the spectrum in the UV range with low losses and spread spectrum. The gain coefficient of Raman g_R is 0.9 x 10^{-13} m/W, and the intensity of the I_p pump is 0.8 x 1014 W/cm^2 [16]. With the value of Is is 5.234 W/m^2 (see section 4.1), the resulting increase in the intensity is:

$$\mathbf{d}\boldsymbol{I}_{\mathbf{s}}/\mathbf{dz} = \boldsymbol{g}_{\boldsymbol{R}}\boldsymbol{I}_{\boldsymbol{P}}\boldsymbol{I}_{\mathbf{S}}$$

$$= 0{,}9 \times 10\text{-}13 \times 0{,}8 \times 1014 \times 5.234$$

$$= 37.684{,}8\ \mathrm{W/m^2}$$

The whole processes occurred in the phase 3 are depicted in Figure 10.

4.4. Processing the Wavelength by The Spectrometer

In the fourth phase, the SO_2 wavelength from the amplifier enters the spectrometer, passes through the slit (1), bandpass filter (2), collimating mirror (3), grating (4), focus mirror (5), until it arrives and is read by the detector (6), as shown in Figure 11.

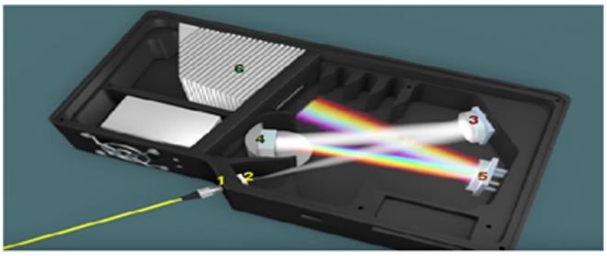

Figure 11. Processing the wavelength by the Spectrometer.

The light intensity that the detector reads, has the unit of W/m^2. As for the unit conversion, using the value I (λ) is:

$$1\ \mathrm{W/cm^2} = 14{,}33\mathrm{gCal/cm^2min}$$
$$37.684{,}8\ \mathrm{W/m^2} = 14{,}33 \times 37.684{,}8 \times 10^{-4}$$
$$= 54{,}0023\ \mathrm{gCal/cm^2s}$$
$$= 0{,}900039\ \mathrm{gCal/cm^2s}$$

Thus, the intensity value read by the detector using the equation results with the assumed values in the previous exposure is 37,684.8 W/m^2 or 0.900039 $gCal/cm^2s$. The example of SO_2 spectrometry is depicted in Figure 12.

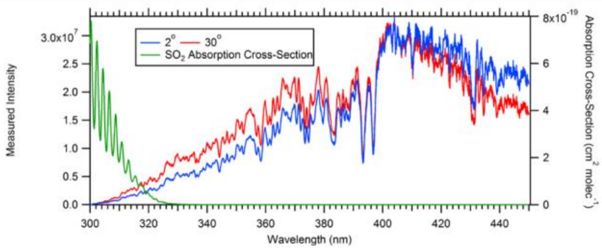

Figure 12. SO2 spectrometry as the analysis result of Spectrometer [17].

5. CONCLUSION

The conclusion that can be drawn from this study is that DOAS uses the spectrum of sunlight or the moon through SO_2 gas to determine the quantity of gas based on the spectrum as well, so that it can be used to monitor the intensity of SO_2 in the Gunung Anak Krakatau vulcanic ashes. The monitoring can be conducted from The PVMBG's Krakatau Monitoring Station at Hargo Pancoran villages (41,19 km from the GAK) by using a catadioptric type optical telescope device and Spectrometer. This study also introduced the deployment of an optical bandpass filter UG11 and a Raman Amplifier, which is expected to improve the spectrum reading accuracy of the DOAS detector the (spectrometer). Based on this study, the real equipment of DOAS is expected to be designed and implemented to monitoring the Gunung Anak Krakatau activity.

REFERENCES

[1] R.D. Cadle, R.D, A comparison of volcanic with other fluxes of atmospheric trace gas constituents, in: Review of Geophysics and Space Physics, v.18 (4), 1980, pp. 746-752. DOI: https://doi.org/10.1029/RG018i004p00746

[2] Liputan6, Gunung Anak Krakatau. Retrieved from https://liputan6.com/tag/gunung-anak-krakatau, 2 October 2018. Accessed on 27 December 2019.

[3] Detiknews, BMKG Pasang 6 Sensor Pantau Aktivitas Gunung Anak Krakatau. Retrieved from https://news.detik.com/berita/d-4358609/bmkg-pasang-6-sensor-pantau-aktivitas-gunung-anak-krakatau, 26 December 2018. Accessed on 27 December 2019.

[4] Okezone TV, BMKG Pasang Alat Pemantau Ketinggian Air untuk Deteksi Dini Tsunami Dekat Gunung Anak Krakatau. Retrieved from https://news.okezone.com/read/2019/02/07/340/-2023283/bmkg-pasang-alat-pemantau-ketinggian-air-untuk-deteksi-dini-tsunami-dekat-gunung-anak-krakatau, 27 Februari 2019. Accessed on 27 December 2019.

[5] A. Bongartz, J. Kames, F. Welter, U. Schurath, Near-UV absorption cross sections and tran/cis equilibrium of nitrous acid, in: *J.Phys Chem*. 95 (3), 1991, pp. 1076-1082. DOI: https://doi.org/10.1021/j100156a012

[6] C. Oppenheimer, S. Bruno, R.S. Martin, Sulfur Degassing From Volcanoes: Source Conditions, Surveillance, Plume Chemistry and Earth System Impacts, in: Reviews in Mineralogy and Geochemistry, Cambridge University, United Kingdom, Vol. 73(1), 2011, pp. 363-421. DOI: https://doi.org/10.2138/rmg.2011.73.13

[7] B. Galle, DORSIVA Project Proposals. Sweden, 2003.

[8] U. Platt, J. Stutz, Differential Optical Absorption Spectroscopy: Principles and applications. Springer-Verlag Heidelberg, 2008. ISBN. 978-3-540-75776-4.

[9] Y. Zhang, Wireless Sensor Network for Volcano Monitoring, Master Thesis, KTH School of Information and Communication Technology (ICT), Microelectronics and Information Technology, Sweden, 2005.

[10] _, Fundamentals of Environmental Measurements, Solar Radiation and Photosynetically, Active Radiation. *Fondriest Environmental, Inc*., 2014. https://www.fondriest.com/environmental-measurements/parameters/weather/photosynthetically-active-radiation/. Accessed on 4 January 2020.

[11] A. Kost, Module 10 - Optical Amplifiers, Center for Integrated Access Network, University of Arizona, 2018. http://data.cian-erc.org/supercourse/undergraduatelevel/module_10/10_SC_Undergraduate_level_Module_10_Kost.pdf. Accessed on 4 January 2020.

[12] I. Rahardjo, I Fitriana, Analisis Potensi Pembangkit Listrik Tenaga Surya di Indonesia, in: Strategi Penyediaan Listrik Nasional Dalam Rangka Mengantisipasi Pemanfaatan PLTU Batubara Skala Kecil, PLTN, Dan Energi Terbarukan, 2010. https://www.oocities.org/markal_bppt/publish/pltkcl/plrahard.pdf. Accessed on 4 January 2020.

[13] D. Blackie, R. Blackwell-Whitehead, G. Stark, J.C. Pickering, P.L. Smith, J. Rufus, A.P. Thorne, High-resolution photo absorption cross-section measurements of SO_2 at 198^0 K from 213 to 325 nm, in: *Journal of Geophysical Research*, VOL. 116(E3), American Geophysical Union, 2011. DOI: https://doi.org/10.1029/2010JE003707

[14] J. Mathew, A. Prakash, M. Sarpotdar, A.G. Sreejith, M. Safnova, J. Murthy, An Ultraviolet imager to study bright UV sources, in: Proc. SPIE 9905, Space Telescopes and Instrumentation 2016: Ultraviolet to Gamma Ray, 990532,18 July 2016. DOI: https://doi.org/10.1117/12.2232977

[15] Schott Data Sheet, UG11. Retrieved from www.sydor.com/wp-content/uploads/2019/06/SCHOTT-UG11-UV-Bandpass-Filter.pdf. Accessed on 4 January 2020.

[16] R. Ramaswami, K.N. Sivarajan, G. Sasaki, Optical Networks. Elsevier ScienceDirect, 2011. DOI: https://doi.org/10.1016/C2009-0-17339-7

[17] Z.Y.W. Davis, R. McLaren, Recommendations for Spectral Fitting of SO2 from MAX-DOAS Measurements, in: Atmospheric Measurements Techniques, EGU, 2020. DOI: https://doi.org/10.5194/amt-2019-420